Seismic Performance Analysis of PVA Steel Hybrid Fiber Reinforced Concrete Columns with Different Axial Compression Ratios

Wen Li, Ruibo Wang*, Tong Wang

School of Civil Engineering, Northeast Petroleum University, Daqing, Heilongjiang, 163318, China

*1607385719@qq.com

Abstract. With the development of materials science and technology, extensive experimental research has been conducted on the properties of PVA steel hybrid fiber-reinforced cement-based composites. However, due to external and human factors, errors and relative limitations have occurred. Therefore, the use of numerical simulation methods can comprehensively reflect the seismic performance of components, providing sufficient basis and reliable theoretical basis for experiments and engineering applications. This article studies the seismic performance of PVA steel HyFRCC columns based on the OpenSEES platform, including the following aspects: using the bond slip model and fiber model considering the bond between steel bars and concrete as the constitutive relationship of PVA steel HyFRCC materials based on the OpenSEES platform, finite element analysis was conducted on PVA steel HyFRCC columns, and compared with experimental results. The results show that compared with the experimental results, the simulated hysteresis curve, skeleton curve, peak bearing capacity, displacement ductility coefficient, and equivalent viscous damping coefficient have smaller errors, indicating that the constitutive model is suitable for studying the seismic performance of PVA steel HyFRCC columns. Based on the OpenSEES platform, the influence of different axial compression ratios on the seismic capacity of PVA steel HyFRCC columns was studied using the above model. The results indicate that as the axial load ratio increases, the stiffness degradation becomes faster, and the energy dissipation performance and ductility gradually decrease.

Keywords: Axial Compression Ratio, Seismic Performance, PVA Fiber, Steel Fiber

1 Introduction

This article studies the seismic performance of four reinforced concrete[1] cross shaped columns, with the same parameters except for axial compression ratio and whether fibers[3] are added. The concrete strength is C50, the column section size is 400mm × 400mm, the protective layer thickness is 35mm, and the effective height of the column

© The Author(s) 2025
Y. Zhang et al. (eds.), *Proceedings of the 2024 10th International Conference on Architectural, Civil and Hydraulic Engineering (ICACHE 2024)*, Advances in Engineering Research 259,
https://doi.org/10.2991/978-94-6463-658-1_11

is 1200mm. Symmetrical reinforcement is selected for the longitudinal load-bearing steel[5] bars of the column, with four HRB400 grade steel bars with a diameter of 16mm and four HRB400 grade steel bars with a diameter of 20mm, with a longitudinal reinforcement ratio[6] of 2.01%; The stirrups are made of HRB335 grade hot-rolled round steel; its diameter is 6.5mm. Simulate the seismic performance of ordinary concrete columns using OpenSEES finite element software[2], and verify the reliability of the model by simulating the constitutive behavior of concrete02 concrete and steel02 steel reinforcement. Validate the seismic performance of the remaining three PVA steel HyFRCC columns using Bond Sp01 constitutive[4] and fiber models, and verify the reliability of the PVA steel HyFRCC column model by comparing hysteresis curves and skeleton curves. Finally, the seismic performance was analyzed using different axial load[7] ratios of 0.5, 0.6, and 0.7, providing sufficient basis and reliable theoretical foundation for experiments and engineering applications.[9]

2 Establishment and Verification of Finite Element Model

2.1 Model Validation

This article establishes a finite element model based on Han Weili's experiment, and calculates and analyzes the model columns in Opensees software. The experimental results are compared with the finite element[4] model analysis results to verify the accuracy of the finite element model. The comparison results are shown in Figure 1, Figure 2 and Table 1.

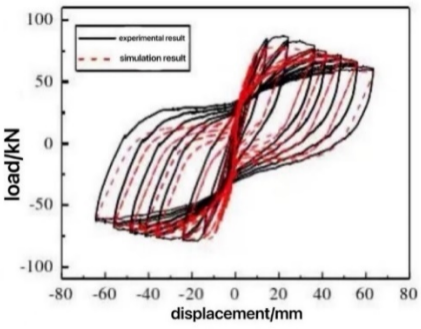

Fig. 1. Comparison of hysteresis curves

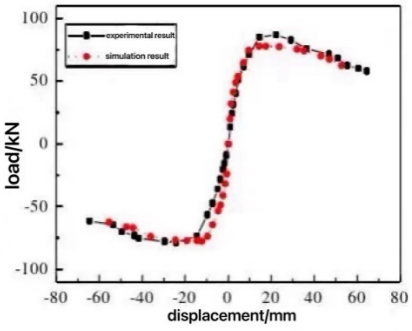

Fig. 2. Comparison of Skeleton Curves

Table 1. RC Column Experimental and Simulated Peak Load

RC Column experiments with the simulated peak loads						
The specimen number	analog value (kN)		trial value (kN)		deviation(%)	
	forward direction	negative direction	forward direction	negative direction	forward direction	negative direction
RC	52.11	51.48	52.72	62.16	1.08	13.4

From Figure 1, the hysteresis curve of the specimen obtained from finite element simulation calculation[1] is in good agreement with the hysteresis curve obtained from the experiment[7] as a whole; The loading and unloading trends, as well as the shape of the hysteresis curve, are basically consistent and in good agreement[10] with the experimental hysteresis curve. However, there is a certain degree of error in the initial stiffness of the two. The initial stiffness of the hysteresis curve simulated by finite element method is greater than that of the experimental hysteresis curve, and there is also a certain difference in the horizontal peak[9] load between the two. The simulated horizontal peak load is slightly higher than the experimental horizontal peak load. It can be seen that adding the consideration of bond slip between steel bars and concrete in the fiber model can better simulate the fullness of the column hysteresis curve[5], and the hysteresis curve is basically consistent with the experimental curve. From Figure 2, it can be seen that the simulated column skeleton curve is consistent with the experimental curve, and its initial elastic and stiffness degradation rates[7] are basically consistent with the test results.

3 The Effect of Different Axial Compression Ratios on Seismic Performance

This section conducts Finite element analysison four PVA steel HyFRCC columns with different axial load ratios[2], based on the OpenSEES platform, study the effect of axial load ratio on the seismic effect of PVA steel HyFRCC columns. The cross-sectional size of the column is 400mm × 400mm, the thickness of the protective layer is 35mm, the effective height of the column is 1200mm, the shear span ratio is 3, and the axial load ratios[1] are 0.4, 0.5, 0.6, 0.7. The cross-sectional dimensions and reinforcement form of the specimen are shown in Figure 3.

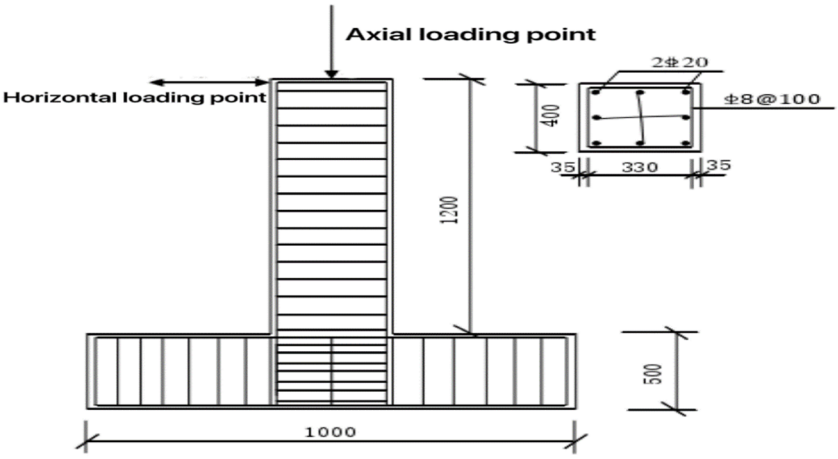

Fig. 3. Sectional dimensions and reinforcement of specimens (unit: mm)

3.1 Hysteresis Curve and Skeleton Curve

Axial compression ratio an important influencing factor about the seismic performance[9] of PVA steel HyFRCC columns. Figure 4 shows the hysteresis curves of four columns with different axial load ratios[6], and Figure 4 shows the skeleton curves[10] of columns with different axial load ratios.

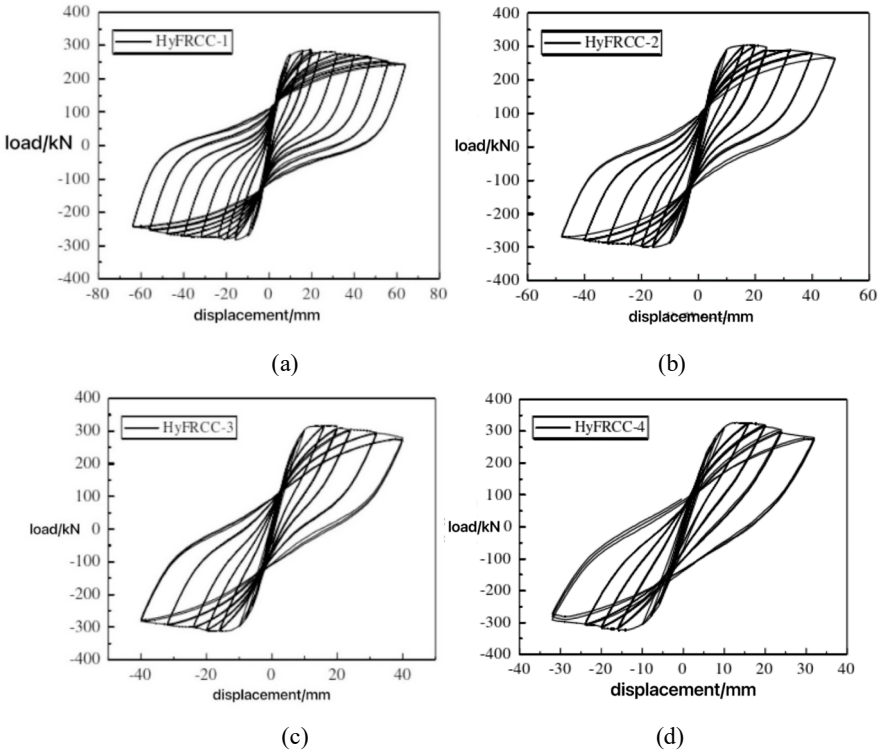

Fig. 4. Comparison of hysteresis curves

Figures 4 (a), (b), (c), and (d) show the hysteresis curves of PVA steel HyFRCC columns under different axial load ratios. At the initial stage of horizontal displacement loading, each specimen has a small horizontal displacement[3] and low stress. The specimens are in the elastic stage with no residual deformation, and the loading and unloading curves almost overlap[5]. As the displacement continues to increase, the slope of the hysteresis curve gradually tilts towards the horizontal axis, the hysteresis loop takes on a curved shape, the surrounding area significantly increases, and the energy dissipation capacity of the specimen gradually increases. After the longitudinal reinforcement yields[2], the number of cycles increases continuously, and the peak load and slope of the curve at the same horizontal displacement both show a slow decrease, indicating that the stiffness degradation phenomenon gradually occurs in the specimen

during the loading and unloading process. From the figure, it can be seen that components with lower axial compression[7] ratios have larger hysteresis curve areas and fuller saturation[9], indicating stronger energy dissipation capabilities.

Table 2. Peak Load of PVA Steel HyFRCC Column

PVA-steel HyFRCC Peak column load					
The specimen number	forward direction		negative direction		negative direction n_1
	peak displacement (mm)	Peak load(kN)	peak displacement (mm)	Peak load(kN)	
HyFRCC-1	19.70	284.04	-21.02	-281.57	0.40
HyFRCC-2	19.12	302.95	-20.20	-301.06	0.50
HyFRCC-3	17.30	314.60	-18.21	-314.52	0.60
HyFRCC-4	14.02	324.62	-15.41	-324.24	0.70

Table 2 shows the peak loads and displacements[3] in both directions of specimens under different axial load ratios. It can be inferred from the data in the table that as the axial load ratio increases, the load bearing capacity[10] of PVA steel HyFRCC columns also increases, but the magnitude of the increase decreases.

4 Conclusions

This article compares the imitate results with test results, verifies the accuracy of the model and the applicability of the constitutive model, and studies the effect of different axial load ratios on the seismic performance[8] of PVA steel HyFRCC columns. The main conclusions are as follows:

1. Finite element analysis was conducted on ordinary concrete columns using OpenSEES software. Establish a model of a regular concrete column using the Concrete 02[7] and Steel 02[7] constitutive models. This model can effectively simulate the saturation degree of the hysteresis curve of concrete columns, and the simulation results have high accuracy.

2. Studied the seismic effects of different axial load ratios on PVA steel HyFRCC columns. The results show that when the axial load ratio is less than 0.6, as the axial load ratio increases, the bearing capacity of the specimen significantly[3] increases, the stiffness degradation rate also accelerates, the hysteresis curve changes less, and the seismic performance is relatively stable. However, when the axial load ratio exceeds 0.6, the enclosed area of the energy dissipation hysteresis curve significantly[4] decreases, and the energy dissipation capacity decreases, which is not conducive to the seismic behavior of the structure.

3. As a new type of material, its constitutive relationship and seismic performance[5] still need further research. This article only conducted finite element analysis on the

seismic behavior of PVA steel HyFRCC columns with different axial load ratios, and further research is needed to investigate the effects of fiber content and loading methods on seismic performance[8].

References

1. Du Ke, Sun Jingjiang, Xu Weixiao Research on Unit, Section and Fiber Division in Fiber Model [J] Earthquake Engineering and Engineering Vibration, 2012, 32 (5): 8
2. Wang Tao, Sun Yan, Meng Liyan Numerical analysis of RC column quasi-static test based on OpenSEES [J] Journal of Heilongjiang University of Science and Technology, 2016, 26 (01): 89-94
3. MALVAR L J, ROSS C A. Review of Strain Rate Influence for Concrete inTension[J]. ACI Mater J, 1998, 95(6): 735-739.
4. Park R, Priestley M, Gill W D. Seismic performance of square-confined concrete columns[J]. Journal of the Structural Division, ASCE. 1982, 108(4): 929-950.
5. Baudouin-M Aissoun, Hwang Soo-Duck, Khayat Kamal-H. Influence of aggregate characteristics on workability of superworkable concrete. MateYials and Structures, 2016, 49(1-2): 597-609.
6. Bu Haifeng, Hu Sikang, Zhang Yaoting, etc A quasi-static numerical analysis model for RC columns based on OpenSees [J] Journal of Civil Engineering and Management, 2016, 33 (05): 21-27+32
7. Zhang Lanfang, Zhong Xun, Liu Qianmin, etc Numerical analogy of low cycle repeated testing of giant SRC columns based on OpenSees [J] Journal of Earthquake Engineering, 2017, 39 (06): 1134-1114
8. Cui Ming, Liu Wenlin, Han Jianping Nonlinear numerical analogy of seismic performance of PVA fiber-reinforced concrete frame columns [J] Low temperature Building Technology, 2017, 39 (10): 39-43
9. Su J, Hu Q, Liu J. Nonlinear numerical analogy of PVA fiber high-strength concrete columns under low cycle repeated loading [J]. IOP Conference Series Earth and Environmental Science, 2017, 61 (1): 012096.
10. Xu Zilong, Xie Qun. Study on the tensile properties of hybrid fiber-reinforced high toughness cement-based composites [J]. Journal of Jinan University (Natural Science Edition), 2021, 35 (01): 68-73

Open Access This chapter is licensed under the terms of the Creative Commons Attribution-NonCommercial 4.0 International License (http://creativecommons.org/licenses/by-nc/4.0/), which permits any noncommercial use, sharing, adaptation, distribution and reproduction in any medium or format, as long as you give appropriate credit to the original author(s) and the source, provide a link to the Creative Commons license and indicate if changes were made.

The images or other third party material in this chapter are included in the chapter's Creative Commons license, unless indicated otherwise in a credit line to the material. If material is not included in the chapter's Creative Commons license and your intended use is not permitted by statutory regulation or exceeds the permitted use, you will need to obtain permission directly from the copyright holder.